The Effect of Recent Admixture on Inference of Ancient Human Population History

Kirk E. Lohmueller,*,†,1 Carlos D. Bustamante†,2 and Andrew G. Clark*

*Department of Molecular Biology and Genetics and †Department of Biological Statistics and Computational Biology,
Cornell University, Ithaca, New York 14853

ABSTRACT

Despite the widespread study of genetic variation in admixed human populations, such as African-Americans, there has not been an evaluation of the effects of recent admixture on patterns of polymorphism or inferences about population demography. These issues are particularly relevant because estimates of the timing and magnitude of population growth in Africa have differed among previous studies, some of which examined African-American individuals. Here we use simulations and single-nucleotide polymorphism (SNP) data collected through direct resequencing and genotyping to investigate these issues. We find that when estimating the current population size and magnitude of recent growth in an ancestral population using the site frequency spectrum (SFS), it is possible to obtain reasonably accurate estimates of the parameters when using samples drawn from the admixed population under certain conditions. We also show that methods for demographic inference that use haplotype patterns are more sensitive to recent admixture than are methods based on the SFS. The analysis of human genetic variation data from the Yoruba people of Ibadan, Nigeria and African-Americans supports the predictions from the simulations. Our results have important implications for the evaluation of previous population genetic studies that have considered African-American individuals as a proxy for individuals from West Africa as well as for future population genetic studies of additional admixed populations.

STUDIES of archeological and genetic data show that anatomically modern humans originated in Africa and more recently left Africa to populate the rest of the world (TISHKOFF and WILLIAMS 2002; BARBUJANI and GOLDSTEIN 2004; GARRIGAN and HAMMER 2006; REED and TISHKOFF 2006; CAMPBELL and TISHKOFF 2008; JAKOBSSON et al. 2008; LI et al. 2008). Given the central role Africa has played in the origin of diverse human populations, understanding patterns of genetic variation and the demographic history of populations within Africa is important for understanding the demographic history of global human populations. The availability of large-scale single-nucleotide polymorphism (SNP) data sets coupled with recent advances in statistical methodology for inferring parameters in population genetic models provides a powerful means of accomplishing these goals (KEINAN et al. 2007; BOYKO et al. 2008; LOHMUELLER et al. 2009; NIELSEN et al. 2009).

It is important to realize that studies of African demographic history using genetic data have come to qualitatively different conclusions regarding important parameters. Some recent studies have found evidence for ancient (>100,000 years ago) two- to fourfold growth in African populations (ADAMS and HUDSON 2004; MARTH et al. 2004; KEINAN et al. 2007; BOYKO et al. 2008). Other studies have found evidence of very recent growth (PLUZHNIKOV et al. 2002; AKEY et al. 2004; VOIGHT et al. 2005; COX et al. 2009; WALL et al. 2009) or could not reject a model with a constant population size (PLUZHNIKOV et al. 2002; VOIGHT et al. 2005). It is unclear why studies found such different parameter estimates. However, these studies all differ from each other in the amount of data considered, the types of data used (e.g., SNP genotypes vs. full resequencing), the genomic regions studied (e.g., noncoding vs. coding SNPs), and the types of demographic models considered (e.g., including migration vs. not including migration postseparation of African and non-African populations).

Another important way in which studies of African demographic history differ from each other is in the populations sampled. Some studies have focused on genetic data from individuals sampled from within Africa (PLUZHNIKOV et al. 2002; ADAMS and HUDSON

2004; Voight *et al.* 2005; Keinan *et al.* 2007; Cox *et al.* 2009; Wall *et al.* 2009), while other studies included American individuals with African ancestry (Adams and Hudson 2004; Akey *et al.* 2004; Marth *et al.* 2004; Boyko *et al.* 2008). While there is no clear correspondence between those studies which sampled native African individuals (as opposed to African-Americans) and particular growth scenarios, it is clear from previous studies that African-American populations do differ from African populations in their recent demographic history. In particular, genetic studies suggest that there is wide variation in the degree of European admixture in most African-American individuals in the United States and that they have, on average, ~80% African ancestry and 20% European ancestry (Parra *et al.* 1998; Pfaff *et al.* 2001; Falush *et al.* 2003; Patterson *et al.* 2004; Tian *et al.* 2006; Lind *et al.* 2007; Reiner *et al.* 2007; Price *et al.* 2009; Bryc *et al.* 2010). Furthermore, both historical records and genetic evidence suggest that the admixture process began quite recently, within the last 20 generations (Pfaff *et al.* 2001; Patterson *et al.* 2004; Seldin *et al.* 2004; Tian *et al.* 2006). Recent population admixture can alter patterns of genetic variation in a discernible and predictable way. For example, recently admixed populations will exhibit correlation in allele frequencies (*i.e.*, linkage disequilibrium) among markers that differ in frequency between the parental populations. This so-called admixture linkage disequilibrium (LD) (Chakraborty and Weiss 1988) can extend over long physical distances (Lautenberger *et al.* 2000) and decays exponentially with time the since the admixture process began (*i.e.*, recently admixed populations typically exhibit LD over a longer physical distance than anciently admixed populations).

While it is clear that African-American populations have a different recent demographic history than do African populations from within Africa and that admixture tracts can be identified in admixed individuals (Falush *et al.* 2003; Patterson *et al.* 2004; Tang *et al.* 2006; Sankararaman *et al.* 2008a,b; Price *et al.* 2009; Bryc *et al.* 2010), the effect that admixture has on other patterns of genetic variation remains unclear. For example, Xu *et al.* (2007) found similar LD decay patterns when comparing African-American and African populations. It is also unclear whether the recent admixture affects our ability to reconstruct ancient demographic events (such as expansions that predate the spread of humans out of Africa) from whole-genome SNP data. Most studies of demographic history have summarized the genome-wide SNP data by allele frequency or haplotype summary statistics. If these summary statistics are not sensitive to the recent European admixture, then the African-American samples may yield estimates of demographic parameters that are close to the true demographic parameters for the ancestral, unsampled, African populations. This would suggest that the differences in growth parameter estimates obtained from African populations cannot be explained by certain studies sampling African-American individuals and others sampling African individuals from within Africa. However, if these statistics are sensitive to recent admixture, then they may give biased estimates of growth parameters.

Here, we examine the effect of recent admixture on the estimation of population demography. In particular, we estimate growth parameters from simulated data sets using SNP frequencies as well as a recently developed haplotype summary statistic (Lohmueller *et al.* 2009). We compare the demographic parameter estimates made from the admixed and nonadmixed populations and find that some parameter estimates are qualitatively similar between the two populations when inferred using allele frequencies. Inferences of growth using haplotype-based approaches appear to be more sensitive to recent admixture than inferences based on SNP frequencies. We discuss implications that our results have for interpreting studies of demography in admixed populations.

METHODS

Demographic model for simulations: For generating simulated data, we used a demographic model that qualitatively approximates the history of African, European, and African-American human populations. We chose to focus on African-American demography as (1) African-American populations are a significant component of the U.S. population (~12%, U.S. Census 2000 Summary File 1, http://factfinder.census.gov) and are, therefore, heavily studied by population and medical geneticists in the United States; (2) there is considerable understanding of the historical context surrounding the recent demographic history of African-Americans including the trans-Atlantic slave trade, early American history, and history of African-American migrations within the United States; and (3) the admixture process in other human populations is likely to be more complex.

Figure 1 shows an illustration of the demographic model considered. Essentially, an ancestral population of size N_B split t_{split} generations ago to form an African population (Pop A) and a European population (Pop E). The African population expanded from its ancestral size (N_B) to its current size (N_A) t_{cur} generations ago. The European population underwent a bottleneck (using parameters similar to those inferred by Lohmueller *et al.* 2009). Note that we assumed no gene flow between Pop A and Pop E after the split even though some studies have found evidence for migration between African and European populations (Schaffner *et al.* 2005; Gutenkunst *et al.* 2009; Nielsen *et al.* 2009; Wall *et al.* 2009). We chose not to include such migration in our models so that our assessments of the effects of recent admixture would not be confounded by
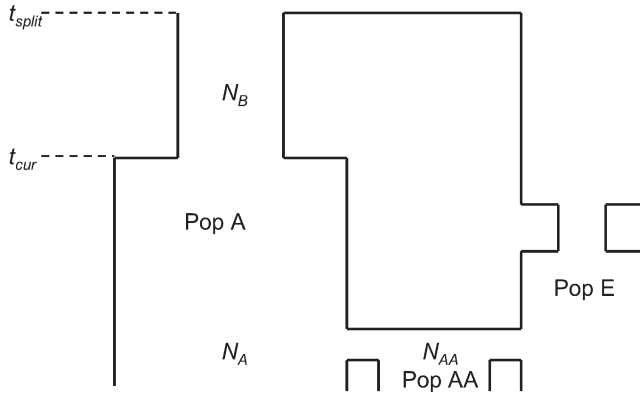
FIGURE 1.—Demographic model for African (Pop A), African-American (Pop AA), and European (Pop E) populations used to simulate test data sets. For all simulations conducted here, $t_{split} = 4000$ generations, $N_A = 20,000$, $N_B = 10,000$, and Pop E followed the bottleneck model from LOHMUELLER *et al.* (2009), except for the ancestral population size (N_B), which was set to 10,000. See text for a further description of the parameters.

other sources of gene flow. Twenty generations ago, the African-American population (Pop AA) was formed and has current size N_{AA} (PFAFF *et al.* 2001; PATTERSON *et al.* 2004; TIAN *et al.* 2006). We assumed 80% of the ancestry of Pop AA comes from Pop A, with the remainder coming from Pop E (PFAFF *et al.* 2001; PATTERSON *et al.* 2004; TIAN *et al.* 2006). Since it is unknown whether there was a founder effect in forming the African-American population, we allowed N_{AA} to vary. All simulations assumed an infinite-sites mutation model and a Wright–Fisher model of reproduction.

Inference on simulated data using the site frequency spectrum: A useful summary of SNP data that potentially contains information regarding the magnitude of recent population growth is the site frequency spectrum (SFS) (FU 1995; GRIFFITHS and TAVARÉ 1998; NIELSEN 2000; WILLIAMSON *et al.* 2005). Mathematically, the SFS is defined for a set of n sequenced chromosomes across S variable sites (*i.e.*, SNPs) as the random vector (X_1, X_2, ..., X_{n-1}), where X_i represents the number of SNPs where the n chromosomes are portioned into exactly i copies of the derived allele and $n - i$ copies of the ancestral allele. For example, X_1 is the number of singleton SNPs in the data, X_2 is the number of SNPs where exactly two chromosomes carry the derived allele, and so on. Note that the sum of the entries in the SFS equals the total number of SNPs in the data set. Informally, one can think of the SFS as a histogram consisting of the number of SNPs at different frequencies in the sample where frequencies are binned at $1/n$ intervals. To determine the accuracy of parameter estimates for N_A, t_{cur}, and N_B/N_A when using the SFS obtained from Pop AA, for each combination of demographic parameters, we simulated 500 data sets, each consisting of 10,000 unlinked 1-kb regions in $n = 24$ chromosomes from each population. The size of each

data set was meant to roughly mimic the scope of resequencing data sets currently in use, such as the Celera Genomics SNP data set (BUSTAMANTE *et al.* 2005; LOHMUELLER *et al.* 2008). We assumed a per-nucleotide mutation rate $\mu = 10^{-8}$ and a per-nucleotide recombination rate, $r = 10^{-8}$. For each data set, we calculated the SFS for both Pop A and Pop AA, which were then used for inference.

To find the maximum-likelihood estimates (MLEs) for the three growth parameters, we used a Poisson likelihood function (see NIELSEN 2000; WILLIAMSON *et al.* 2005; BOYKO *et al.* 2008 for details). Briefly, the observed number of SNPs in each bin, X_i, of the SFS is treated as a Poisson random variable,

$$\Pr(X_i = k \mid \Theta) = e^{-\lambda_i}\lambda_i^k/k!, \qquad (1)$$

where the rate parameter of the Poisson distribution λ_i is the expected number of SNPs in the particular bin of the SFS based on the set $\Theta = \{\theta, \upsilon, \tau\}$ of mutation rate ($\theta = 4N_A\mu$) and growth ($\upsilon = N_B/N_A$; $\tau = t_{cur}/2N_A$) parameters. This expectation has the form where the mutation rate acts as a scaling factor for each data set, so we can rewrite as the product as

$$\lambda_i = E(X_i \mid \Theta) = \theta F(i \mid \upsilon, \tau), \qquad (2)$$

where $F(i \mid \upsilon, \tau)$ is proportional to the number of SNPs at frequency i/n in the sample and can be found either by coalescent simulations (NIELSEN 2000) or via diffusion-based approximations (WILLIAMSON *et al.* 2005). All SNPs and bins of the SFS are treated independently and the final log-likelihood for a given set of growth parameters is the sum of the Poisson log-likelihoods for each bin of the SFS as given below:

$$l(\Theta \mid x) = -\theta \sum_{i=1}^{n-1} F(i \mid \tau, \upsilon) + \sum_{i=1}^{n-1} x_i \log(\theta F(i \mid \tau, \upsilon)). \quad (3)$$

This is a reasonable approximation to the true log-likelihood and holds when there is ample recombination among SNPs. Since the expected values of the SFS entries are not affected by recombination, when applied to linked data, the above inference scheme can be thought of as a composite-likelihood approach (ZHU and BUSTAMANTE 2005; BOYKO *et al.* 2008).

We used the program PRFREQ (BOYKO *et al.* 2008) to find the expected SFS for a given set of growth parameters using the Poisson, rather than the multinomial, implementation. Here we set $\mu = 0.1$, which was the true value used in the simulations to generate the data (10^{-8} per nucleotide $\times$ 10^3 nucleotides per region $\times$ 10^4 regions). To optimize the likelihood function, we found the expected SFS for each parameter combination on a three-dimensional grid (N_A, t_{cur}, and N_B/N_A) of parameter values. It should be noted that the grids used are coarser than those used on real data sets.

Inference on simulated data using the haplotype-count number statistic: Lohmueller *et al.* (2009) recently suggested a new summary statistic for genome-wide SNP data based on haplotype patterns. Their statistic, termed the haplotype-count number (HCN) statistic, is a two-dimensional histogram containing the joint distribution of the number of haplotypes and count of the most common haplotype in windows across the genome. To determine whether we could accurately estimate N_A, t_{cur}, and N_B/N_A when using the HCN statistic obtained from Pop AA, for each combination of demographic parameters, we simulated 100 data sets, each consisting of 7000 unlinked 250-kb regions in $n = 46$ chromosomes from each population. Importantly, as in Lohmueller *et al.* (2009), we used only a random subset of 20 SNPs from each simulated window with minor allele frequency (MAF) >10%. The size of these data sets is meant to mimic the large-scale genotyping surveys currently in use, such as that of Perlegen Sciences, where only a subset of SNPs in the population have been discovered and genotyped (Hinds *et al.* 2005). We assumed a per-nucleotide mutation rate $\mu = 10^{-8}$ and a per-nucleotide recombination rate $r = 10^{-8}$. For each data set, we calculated the HCN statistics for Pop A and Pop AA, which were then used for inference.

To find the MLEs of the three demographic parameters from each data set via the HCN statistic, we used the approach of Lohmueller *et al.* (2009). Briefly, we used a multinomial approximate-likelihood function where the observed number of windows with i haplotypes and where the most common haplotype is at count j come from a multinomial distribution whose parameters are determined by the recombination rate and demographic parameters. We used coalescent simulations to find the parameters for the multinomial distribution for a given set of demographic parameters and recombination rates. Importantly, we fixed the recombination rate in these simulations equal to the true value used to generate the test data sets. The likelihood function was optimized using a grid search.

Analysis of National Institute of Environmental Health Sciences data: We fitted a growth model to the SFS of the Yoruba and African-American samples from the National Institute of Environmental Health Sciences (NIEHS) data (Livingston *et al.* 2004). The Yoruba sample contained $n = 12$ individuals from Ibadan, Nigeria and the African-American sample contained 15 individuals sampled from the United States. We used only noncoding SNPs and excluded SNPs that had genotypes for <10 individuals in at least one of the two populations. Since some SNPs did not have a genotype at every individual, we used the hypergeometric distribution to find the expected SFS for a sample size of 20 chromosomes (Nielsen *et al.* 2004). In total our analysis included 13,588.4 SNPs in the African-American population and 13,487.9 SNPs in the Yoruba population after projection to a sample size of 20 chromosomes. The projection and subsequent analyses were done on the African-American and Yoruba samples separately. For the analysis of the NIEHS data, we used the folded SFS. The folded SFS tabulates the frequency of the minor allele, rather than the derived allele. The folded SFS still contains substantial information regarding demography without having to accurately infer the ancestral/derived states of SNPs (Adams and Hudson 2004).

We estimated the growth parameters for the Yoruba and African-American data sets using the PRFREQ program (Boyko *et al.* 2008). As we did for the analysis of the simulated data sets, we used the Poisson likelihood function. This procedure required an accurate estimate of the per-nucleotide mutation rate, μ. To estimate μ, we used the level of human–chimp divergence at the regions sequenced and the relationship $K = 2T\mu$, where K is the number of human–chimp differences (per nucleotide) and T is the human–chimp divergence time in units of generations. There were 51,770 differences in the 4,644,887 nucleotides sequenced in the builds of the human (hg18) and chimpanzee (pantro2) genomes, giving $K = 0.01114559$ per nucleotide. Then, assuming a human–chimp divergence time of 6 million years, and 25 years/generation, $\mu = (0.01114559 \times 25)/(2 \times 6 \times 10^6) = 2.32 \times 10^{-8}$ per nucleotide/generation. Since before the hypergeometric projection of the SNP frequencies, 7.83% of SNPs were excluded because they contained genotypes for <20 chromosomes in either one population or both populations, we decreased the total number of nucleotides sequenced by the same amount. This led to 4,281,191 total nucleotides that were used for analysis. We again used a grid search to optimize the likelihood function. Profile log-likelihood curves were used to calculate 95% confidence intervals (C.I.'s) for each parameter. We note that fixing of μ to a particular value does not alter the coverage properties for scaled parameters due to the invariance principle of maximum-likelihood inference (Pawitan 2001).

Analysis of the Perlegen data: We fitted a growth model to the African-American sample analyzed by Perlegen Sciences (Hinds *et al.* 2005) using the HCN statistic. We chose to use the Perlegen data rather than other data sets, such as HapMap, because Perlegen genotyped all SNPs that they discovered, without regard to LD status, making subsequent analyses simpler (Lohmueller *et al.* 2009) and relatively free of the ascertainment biases in HapMap.

We divided the genome into nonoverlapping 0.25-cM windows and selected 20 SNPs from each window to construct the HCN statistic. Note that we selected only SNPs with MAF >10% in both the African-American and European-American data sets. Additionally, SNPs that were discovered using fewer than eight chromosomes were not included in the analysis. In total, the
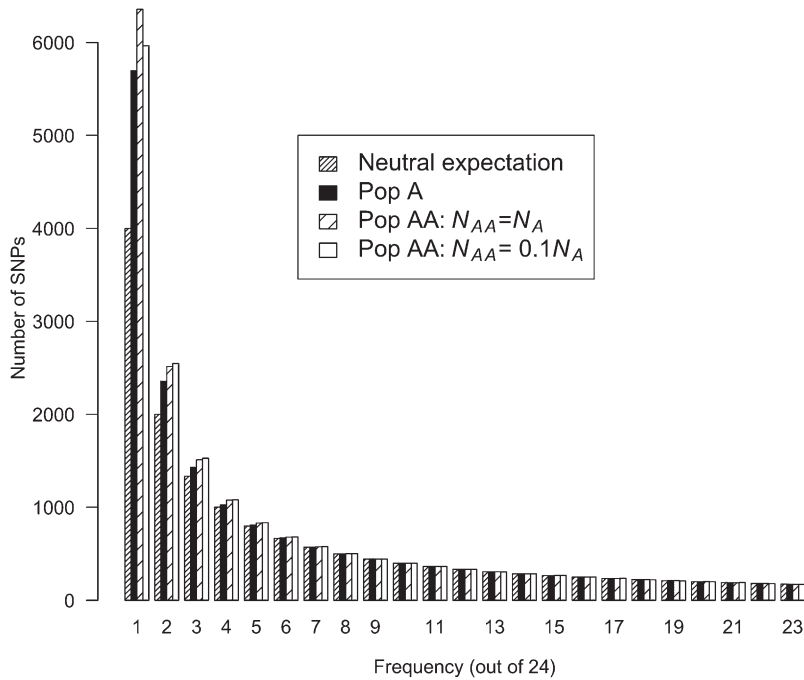
FIGURE 2.—Expected SFS in a sample size of 24 chromosomes for Pop A and Pop AA under population growth. Note the excess of low-frequency SNPs relative to the neutral prediction (FU 1995) in all populations as well as the more pronounced excess of low-frequency SNPs in Pop AA relative to Pop A. $N_A = 20{,}000$; $N_B/N_A = 0.5$; $t_{cur} = 2400$ generations.

HCN statistic contained 8174 windows. As in LOHMUELLER *et al.* (2009), we used Clark's phasing algorithm (CLARK 1990) to infer haplotype phase of the SNP data.

In the coalescent simulations used to generate the expected HCN statistic for a given demographic model, we also phased the simulated data using Clark's phasing algorithm and drew the recombination rate for each simulated region from a gamma distribution to allow for errors in the estimated genetic map (LOHMUELLER *et al.* 2009). Finally, we used the Schaffner recombination hotspot model (SCHAFFNER *et al.* 2005) as implemented in LOHMUELLER *et al.* (2009).

RESULTS

Effect of admixture on patterns of polymorphism: Figure 2 shows the expected SFS for Pop A with twofold growth as well as for Pop AA under two different values of N_{AA}. First, we note there is an excess of low-frequency SNPs in Pop A compared to the neutral prediction. This result is expected since an excess of low-frequency SNPs is a signature of the population expansion (TAJIMA 1989a; SLATKIN and HUDSON 1991). For Pop AA, when $N_{AA} = N_A$, there is an even more pronounced excess of singleton and doubleton SNPs over what is seen in Pop A. However, the remaining bins of the SFS are similar for Pop A and Pop AA. When $N_{AA} = 0.1N_A$, we observe a decrease in the number of singleton SNPs compared to when $N_{AA} = N_A$. However, the number of singleton SNPs with $N_{AA} = 0.1N_A$ is still slightly greater than that for Pop A alone. We also examined the SFS when Pop AA was formed 7 generations ago (PRICE *et al.* 2009) instead of 20 generations ago, corresponding to more recent admixture (supporting information, Figure S1). When

$N_{AA} = N_A$, the SFS for the two different admixture times are indistinguishable. When $N_{AA} = 0.1N_A$, more recent admixture results in a slight increase in the number of singletons, presumably since the more recent founding of Pop AA results in less drift in Pop AA. However, the number of singletons here is still lower than that seen in Pop AA when $N_{AA} = N_A$. Thus, for the parameter combinations investigated here, the SFS for Pop A and Pop AA all appear to have an excess of low-frequency SNPs, with the excess being more pronounced in Pop AA.

We also investigated the effect of recent admixture on the HCN statistic. Figure 3 shows the HCN statistics for simulated data under the three models described above (Pop A; Pop AA, $N_{AA} = N_A$; and Pop AA, $N_{AA} = 0.1N_A$). For Pop AA, when $N_{AA} = N_A$, there is a slight excess (compared to Pop A) of windows that have few haplotypes and a more pronounced excess (again, compared to Pop AA) of windows having the most common haplotype at higher frequency. This pattern likely stems from the fact that some individuals in the admixed population have haplotypes that recently came from Pop E. Since Pop E underwent a bottleneck, it contains less haplotype diversity than Pop A. Thus, the Pop E haplotypes create a shift toward more windows with fewer haplotypes and where the most common haplotype is at higher frequency in the HCN statistic from Pop AA. When $N_{AA} = 0.1N_A$, the difference between the HCN statistics in Pop A and Pop AA becomes even greater due to the loss of haplotypes during the founding of Pop AA. We also examined the HCN statistic when Pop AA was formed 7 generations ago (PRICE *et al.* 2009) instead of 20 generations ago (Figure S2). When $N_{AA} = N_A$, the HCNs for the two
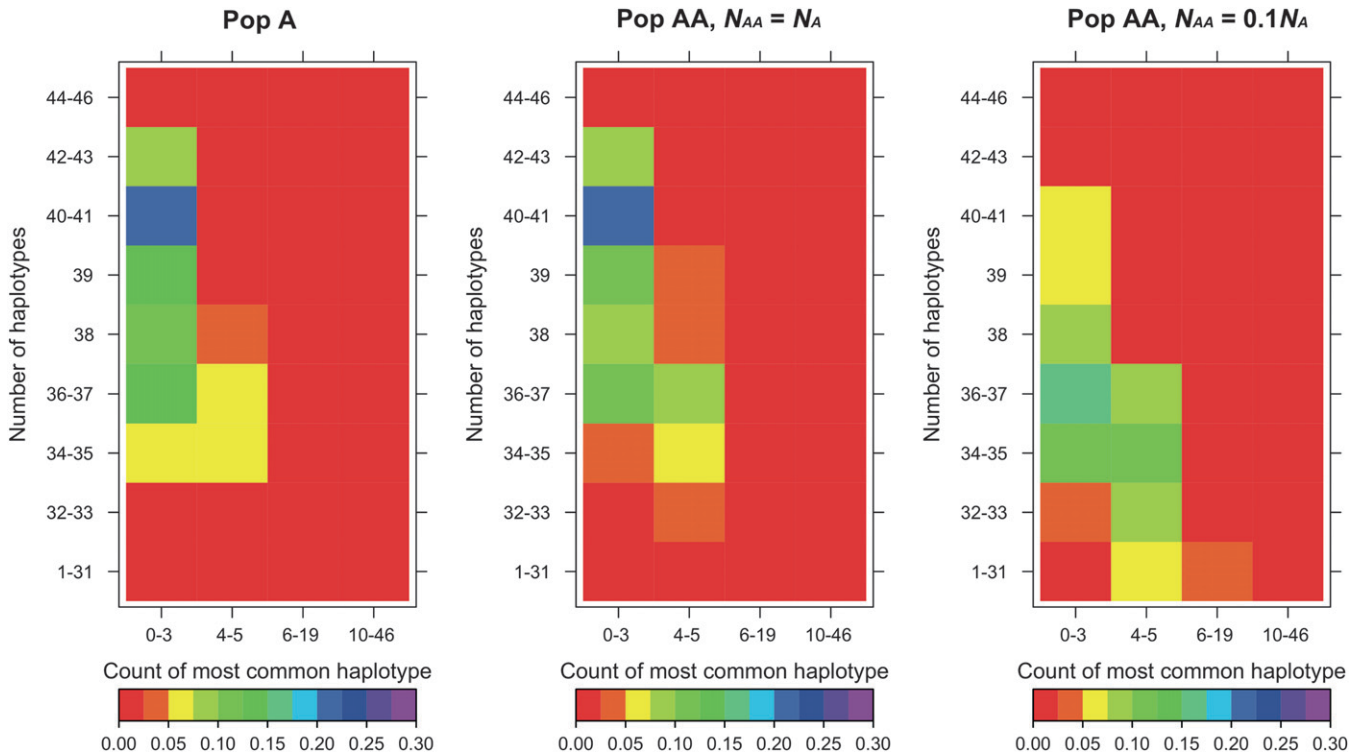
FIGURE 3.—Expected HCN statistics for Pop A and Pop AA. Each cell in the matrix is colored according to the proportion of simulation replicates (windows) having the particular configuration of the number of haplotypes and count of the most common haplotype. For example, red cells contain <2.5% of windows and medium-blue cells contain 20–22.5% of simulated windows. Note the excess of windows with fewer haplotypes and where the most common haplotype is at higher frequency in Pop AA relative to Pop A. This is most pronounced when $N_{AA} = 0.1N_A$. Note that the simulations assume $N_A = 20,000$, $N_B/N_A = 0.5$, and $t_{cur} = 2400$ generations.

different admixture times are nearly identical. When $N_{AA} = 0.1N_A$, overall haplotype diversity is still lower than that seen in Pop AA when $N_{AA} = N_A$; however, the shift is less pronounced than when the admixture and founding occurred 20 generations ago. In summary, the admixture process alters the HCN statistic in a manner that is heavily influenced by the current size of Pop AA and the relative duration of the founder effect forming Pop AA.

Inference of demography from simulated data: To determine whether the differences in the SFS and HCN statistics from Pop A and Pop AA (Figures 2 and 3 and Figure S1 and Figure S2) are meaningful, we estimated the parameters for a population growth model using the SFS and HCN statistics from Pop A and Pop AA (see METHODS). The purpose of this analysis was to see if, using data from Pop AA, we could accurately estimate the current population size of Pop A (N_A), the time of population growth in Pop A (t_{cur}), and the magnitude of population growth (N_B/N_A).

Figure 4A shows the distribution of MLEs inferred using the SFS for the three growth parameters when $t_{cur} = 2400$ generations. For Pop A, the MLEs for all three parameters are clustered at the true parameter values. For Pop AA, when $N_{AA} = N_A$, N_A is slightly overestimated and N_B/N_A is underestimated. The reverse pattern is seen when $N_{AA} = 0.1N_A$. Here, N_A is slightly

underestimated, but N_B/N_A is slightly overestimated. Importantly, in both cases, when using the SFS from Pop AA, all the estimates for N_A are within 10,000 of the true value and all the estimates for N_B/N_A are within 0.15 of the true value. The estimates of the timing since the instantaneous growth event (t_{cur}) present a different pattern. For both models of Pop AA, t_{cur} is severely overestimated (see below).

Figure 4B shows the distribution of the MLEs inferred using the HCN method. Again, the MLEs from Pop A are clustered around the true parameter values. Unlike the estimates made using the SFS, the MLEs from Pop AA are now quite far from the true parameter values. For example, when $N_{AA} = N_A$, N_A is severely overestimated, and N_B/N_A is underestimated. When $N_{AA} = 0.1N_A$, haplotype diversity is lost, leading to the underestimation of N_A when using individuals sampled from Pop AA. Interestingly, t_{cur} is underestimated in both cases.

We also analyzed additional simulated data sets where $t_{cur} = 4000$ generations. Figure 5 shows the distribution of the MLEs inferred using the SFS (Figure 5A) and the HCN statistic (Figure 5B). Note that when estimating parameters using the SFS, the estimates made from Pop AA again approximate the true parameter values for Pop A. In particular, t_{cur} is not as severely overestimated compared to the case where $t_{cur} = 2400$ generations.
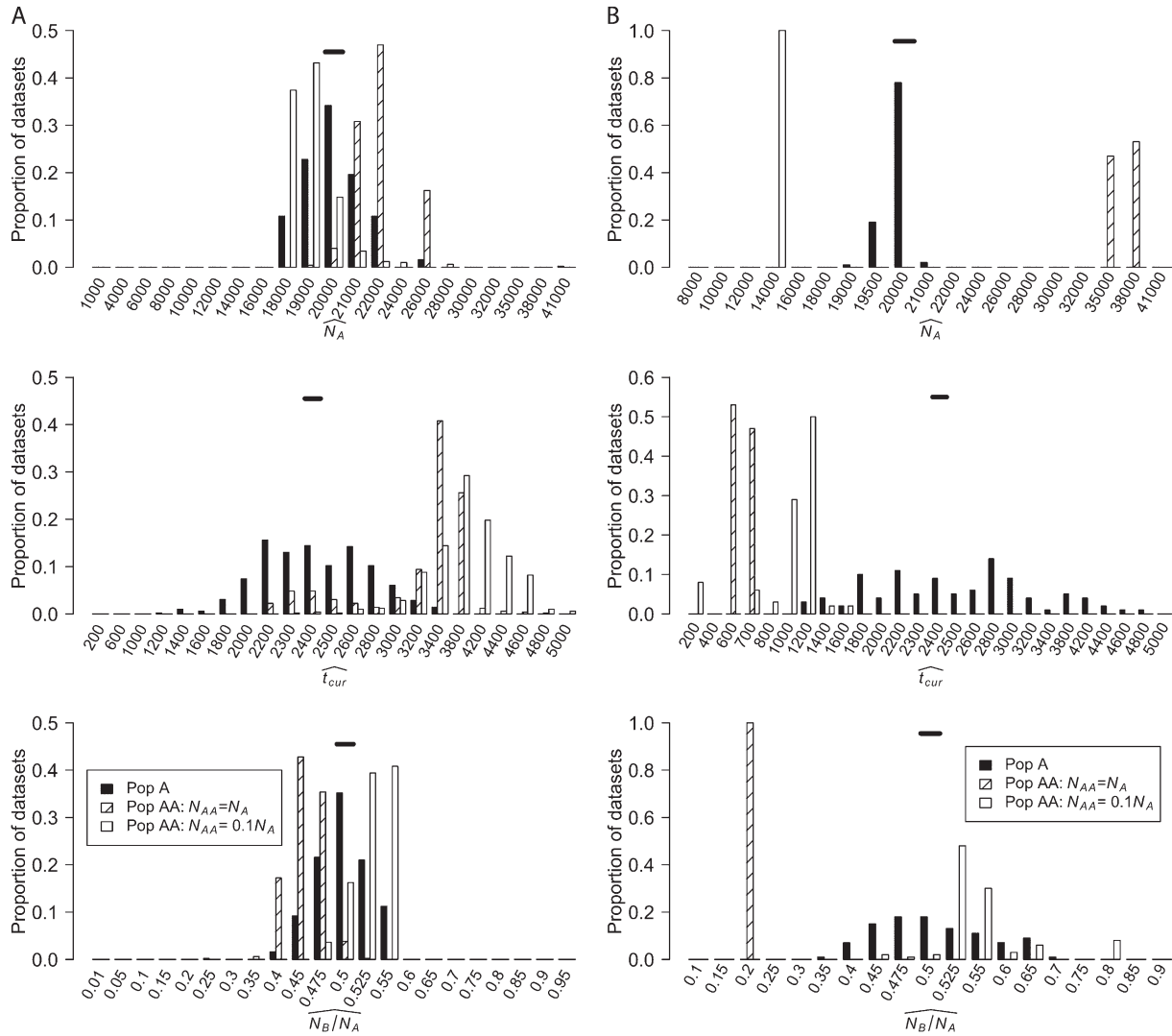
FIGURE 4.—Distribution of MLEs for the three growth parameters inferred using (A) the SFS and (B) the HCN method (see text). Solid horizontal bars denote the true parameter values ($N_A = 20,000$; $N_B/N_A = 0.5$; $t_{cur} = 2400$ generations).

This is especially noticeable when $N_{AA} = N_A$. Thus, part of the explanation for the overestimate of t_{cur} using Pop AA when $t_{cur} = 2400$ generations is that the estimate was heavily influenced by the population "expansion" that occurred at t_{split}, when Pop E and Pop A split (STADLER *et al.* 2009). When $t_{cur} = t_{split}$, this overestimate is less pronounced, although it is still present.

Figure 5B shows that the MLEs inferred using the HCN statistic on individuals from Pop AA are again very far from the true growth parameter values in Pop A. Interestingly, the MLEs of the growth parameters inferred from Pop AA when $t_{cur} = 4000$ are very similar to those inferred when $t_{cur} = 2400$ (compare Figure 4B to Figure 5B). This suggests that the admixture process has such a profound influence on the haplotype patterns that changes in the timing of growth in the parental population cannot be detected using individuals from Pop AA. The current size of Pop AA (N_{AA}), on the other hand, has a large impact on the haplotype

patterns (compare Pop AA, $N_{AA} = N_A$, to Pop AA, $N_{AA} = 0.1N_A$ in Figure 4B). These results, taken together, indicate that recent admixture affects haplotype summary statistics more than it affects the SFS.

Frequently when researchers fit a demographic model to the observed SFS, they will also perform a goodness-of-fit (GOF) test to determine if the best-fitting model can explain the observed SFS (see, for example, ADAMS and HUDSON 2004; CAICEDO *et al.* 2007; BOYKO *et al.* 2008; NIELSEN *et al.* 2009). Given that the simple growth model is the wrong model for Pop AA (the true model involves growth and admixture), we assessed how well the MLEs of the growth parameters generated SFS that fit the observed SFS. Put another way, if a researcher were to fit a growth model to the SFS from an admixed population, how likely is it that the researcher would reject the simple growth model as an explanation for the observed SFS? We performed a simple chi-square GOF test for a particular demo-
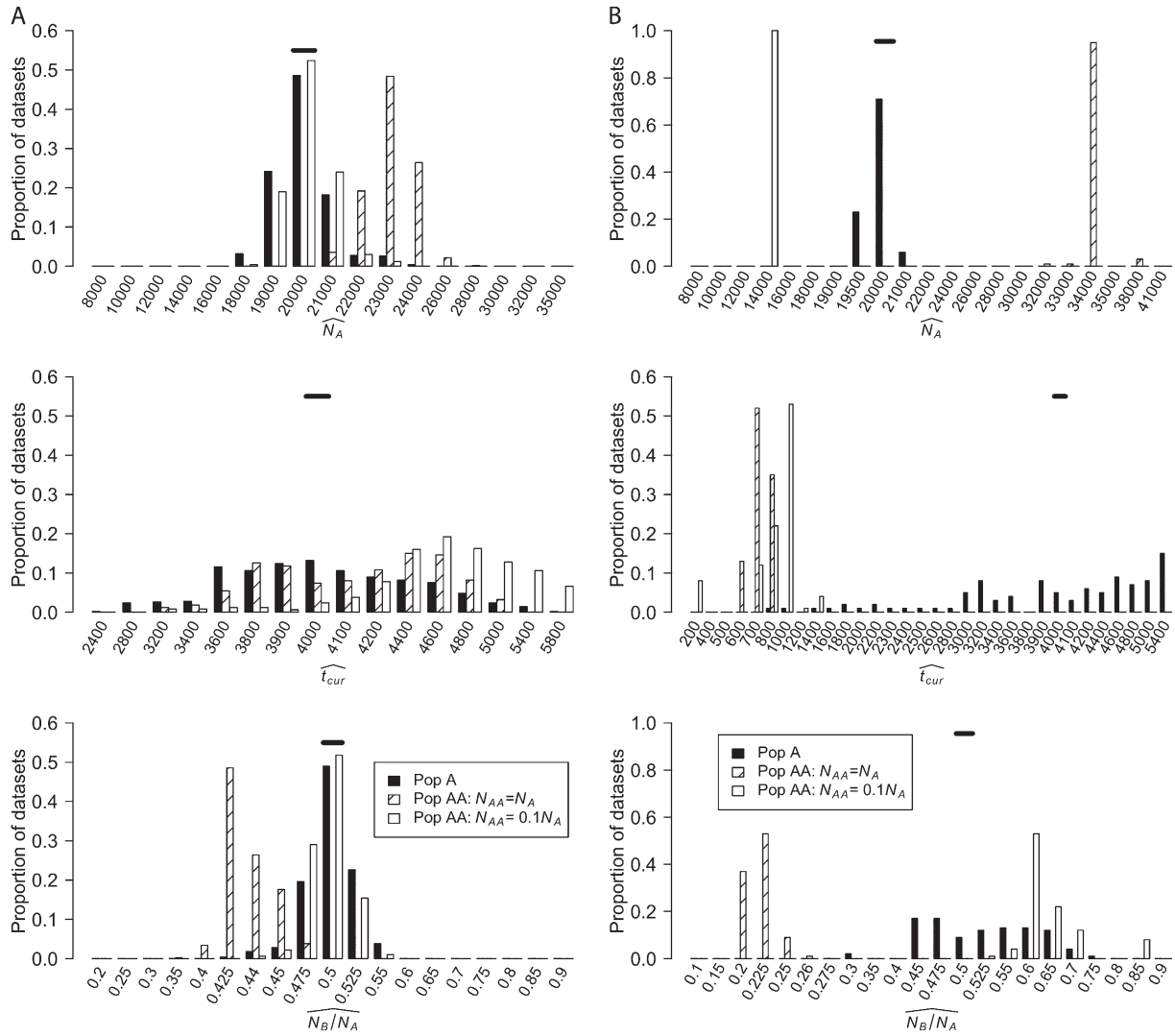
FIGURE 5.—Distribution of MLEs for the three growth parameters inferred using (A) the SFS and (B) the HCN method (see text). Solid horizontal bars denote the true parameter values ($N_A = 20,000$; $N_B / N_A = 0.5$; $t_{cur} = 4000$ generations).

graphic model where we compared the observed SFS in each of the 500 simulated data sets to the expected SFS at the MLEs. Figure S3 shows a quantile–quantile (Q-Q) plot comparing the GOF P-values from Pop AA to those for Pop A. When $t_{cur} = 2400$, there is a shift toward smaller P-values in Pop AA compared to Pop A (Figure S3). This effect is less pronounced when $t_{cur} = 4000$ (Figure S4). We find that when $t_{cur} = 2400$, 5% of the simulated data sets in Pop A have a P-value <0.014. Note that the fraction of data sets with $P < 0.014$ is >1.4% due to the fact that some SNPs are linked, thus reducing the effective number of SNPs. Thus, we use 0.014 as an ~5% rejection region for the GOF test. Using this calibration, we find that 8.8 and 5.8% of data sets for Pop AA have a P-value <0.014, for $N_{AA} = N_A$ and $N_{AA} = 0.1N_A$, respectively. When $t_{cur} = 4000$, 5% of the simulated data sets from Pop A have a P-value <0.0117 compared to 5.6 and 4.8% for $N_{AA} = N_A$ and $N_{AA} = 0.1N_A$, respectively. These results suggest that there is a

slightly worse GOF for the admixed population (Pop AA) than for the nonadmixed population, but we cannot exclude the possibility that some of this pattern may be due to differences in how accurately we optimized the likelihood function across different models. Nevertheless, for the data sets simulated here (containing ~17,000 SNPs), the vast majority (91–95%) of data sets from Pop AA will be unable to reject the pure growth model.

Inference of demography from human data: We estimated the three growth model parameters (t_{cur}, N_A, N_B/N_A) for the African-American and Yoruba populations using the SFS generated from the NIEHS resequencing data set (LIVINGSTON et al. 2004). We chose to use this data set since it was generated by complete resequencing of the same genomic regions in both African-American and Yoruba individuals. As such, we can directly measure the effect that admixture has on estimates of the growth model parameters estimated from the SFS by comparing the parameter estimates

from the two populations. Importantly, since the same regions were studied and the resequencing was done by the same laboratory for the two populations, any differences in the estimates should not be attributable to differences in selective pressure or laboratory errors.

As expected on the basis of the analysis of simulated data described above, the folded SFS of the African-American and Yoruba samples are fairly similar to each other ($P = 0.09$; $\chi^2 = 15.02$; 9 d.f.; Pearson's chi-square test), but the African-American SFS has slightly more low-frequency SNPs and more SNPs overall (see also Figure S5). Using the SNPs in the folded SFS, Wattersons's $\theta = 8.88 \times 10^{-4}$ per nucleotide in the Yoruba sample and 8.95×10^{-4} per nucleotide in the African-American sample. The average number of pairwise differences (π) per nucleotide is 7.99×10^{-4} in the Yoruba sample and 7.93×10^{-4} in the African-American sample. We then estimated the three demographic parameters for the African-American and Yoruba data sets (see METHODS). Figure 6 shows the profile-likelihood curves for the three parameters. The estimate of N_A is slightly higher in the African American population (15,732) compared to the Yoruba population (14,647). However, N_B/N_A is slightly lower in the African-American (0.46) than in the Yoruba (0.5) sample. The profile-likelihood curves overlap substantially for t_{cur}, with a MLE of 5208 generations in the African-American sample and 5425 generations in the Yoruba sample. Importantly, for all three parameters, the $\sim$95% C.I.'s from the profile-likelihood curves ($<$1.92 log-likelihood units) overlap between the African-American and Yorbua estimates, suggesting that the parameter estimates from the two populations are not significantly different from each other.

We then estimated the growth parameters for the Perlegen African-American data set (HINDS *et al.* 2005), using the HCN approach (see METHODS). Figure 6 also shows the profile-likelihood curves for the three parameters. The estimate of N_A (12,500) is slightly smaller than the estimates obtained from the SFS-based analysis. However, the estimates of the other two parameters using the HCN method are quite discordant with the estimates found using the SFS. N_B/N_A is much larger (0.94) when estimated using the HCN than the SFS (0.46). The timing of growth, t_{cur} is also estimated to be much more recent when using the HCN compared to the SFS. Thus, as predicted by the analysis of simulated data sets described above, the HCN method gives different growth parameter estimates than the SFS method when the population has an admixed demographic history.

DISCUSSION

We have examined how recent admixture affects estimates of population growth when using the SFS and the HCN statistic for inference. For certain parameter combinations, we find that growth parameter estimates made using the SFS in the admixed population are qualitatively similar to the true growth parameters from the unadmixed population. This pattern holds more often for the current population size (N_A) and magnitude of growth parameter (N_B/N_A) than for the timing since the growth parameter (t_{cur}) and seems to be little affected by whether or not the admixed population experienced a reduction in size during its founding. If growth occurs at the time the ancestral populations split from each other (*e.g.*, $t_{cur} = t_{split}$ in Figure 1), then estimates of t_{cur} from the admixed population exhibit smaller bias. The HCN approach, on the other hand, is severely affected by recent admixture for all parameters investigated.

Our simulations provide some intuition as to why the SFS and the HCN statistic are differently affected by recent admixture. This difference stems from the manner in which the 20% of ancestry from Pop E affects the SFS and the HCN statistic. The SFS from the admixed population (Pop AA) contains more SNPs and more low-frequency SNPs than does the SFS from the nonadmixed population (Pop A). This is due to the fact that Pop E contains some population-specific SNPs not present in Pop A that are then brought into Pop AA during the admixture process. On the basis of the model assumed here, as well as the analysis of the NIEHS resequencing data, the extra SNPs brought into the admixed population from Pop E do not substantially alter estimates of the population growth parameters. Conversely, the HCN statistic from the admixed population (Pop AA) is shifted toward a higher proportion of windows with fewer haplotypes and where the most common haplotype is at higher frequency than in the nonadmixed Pop A. Essentially, this suggests that there is less haplotype diversity in Pop AA than in Pop A. This pattern arises because $\sim$20% of chromosomes in Pop AA are from Pop E, rather than from Pop A. Since Pop E has undergone a population bottleneck, it has less haplotype diversity than Pop A does. Consequently, Pop AA has lower haplotype diversity than Pop A simply because it contains $\sim$20% of its chromosomes from the populations with lower haplotype diversity (Pop E) while Pop A contains 0% of its chromosomes from the population with lower diversity. Put another way, a single chromosome sampled from Pop A is more likely to represent a new haplotype in a sample from Pop A than a single chromosome sampled from Pop E would. This is the opposite of what was seen for single SNPs, where sampling chromosomes from a mixture of Pop A and Pop E results in an increase in the number of SNPs compared to sampling only Pop A (PTAK and PRZEWORSKI 2002; STADLER *et al.* 2009). This difference indicates that these two summaries of SNP data capture different and complementary aspects of ancestral history.

Due to the sensitivity of haplotype-based approaches to the admixture process, these methods may be more
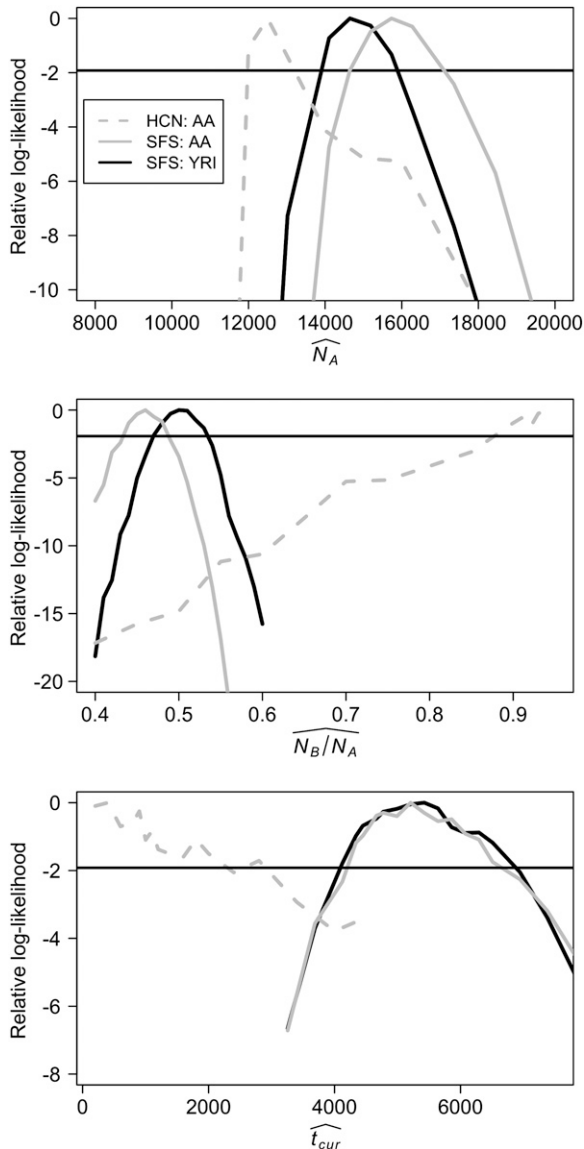
Figure 6.—Profile log-likelihood curves for the three growth model parameters estimated using the SFS from the NIEHS resequencing data for the African-American (AA) and Yoruba (YRI) samples and the HCN statistic from the Perlegen SNP genotype data for the African-American (AA) sample. Note that the two estimates based on the SFS (solid curves) are very similar to each other. The horizontal line in each part denotes the approximate asymptotic 95% C.I.

informative than SFS-based methods for inferring the extent of recent admixture and detecting founder effects associated with admixture. However, when using haplotype-based approaches, researchers need to explicitly model the admixture process, rather than fitting a simplified growth model. Fitting a simple growth model to an admixed population using haplotype patterns will likely give erroneous results. This conclusion does not imply that one method of inference is superior to the other. Instead, the two methods are complementary and the best approach to be used depends then on what one wishes to learn from the data.

Another interpretation for the lack of sensitivity of the SFS-based method to recent admixture is that the SFS-based approach does not have sufficient power to detect when data were drawn from a more complex model. Our results suggest that LD and haplotype patterns as summarized by the HCN statistic are especially sensitive to recent admixture and may provide better diagnostics for detecting ill-fitting models than the SFS alone. Pairwise LD patterns have recently been used by Hernandez et al. (2007) and Gutenkunst et al. (2009) on large-scale macaque and human resequence data sets to assess the fit of the demographic models estimated from the SFS. A similar approach may also provide a means of rigorously assessing model fit for demographic inference from admixed populations.

Since a plethora of genome-wide resequencing data will soon be available from a variety of human populations, we explored the performance of the SFS to estimate growth parameters using a larger data set from Pop AA. We found that increasing the number of chromosomes sampled from 24 to 100 in Pop AA still gave parameter estimates qualitatively similar to those from the smaller data sets (Figure S6), albeit with lower variance. Applying GOF tests to these data, 21% of data sets rejected GOF for the best-fitting model when we thinned the number of SNPs to match that in the smaller data set and 33% rejected GOF when we did not thin the number of SNPs. Thus, not surprisingly, the SFS generated from larger samples increases the power to reject GOF for an incorrect model. However, our results caution that as data sets grow, many may reject GOF due to minor model misspecifications, while still providing qualitatively reasonable estimates of important parameters. Since all models are simplifications of reality, and the sizes of genetic variation data sets are rapidly expanding, this may be an important practical problem in the near future. GOF tests based on the SFS from large data sets should be carefully interpreted while keeping this fact in mind.

While we examined complex demographic models involving population splits, bottlenecks, growth, and admixture, our models are still an oversimplification of the true demography of African and African-American populations. Due to the many parameters in our model, we examined only a few illustrative examples and did not evaluate systematically the effect of changing different parameters. For example, we assumed that the admixture event occurred 20 generations ago and that all Pop AA individuals have, on average, 80% of their ancestry from Pop A. In reality, both these parameters vary among individuals (Pfaff et al. 2001; Patterson et al. 2004). Thus, our models should be taken as illustrative examples of the effect of admixture on inference of ancient growth. It is unclear if the general trends seen from our simulations will hold under more complex models of demography. However, a more recent admixture time (7 generations instead of

20 generations) gave SFS that were qualitatively similar to those found when admixture occurred 20 generations ago (compare Figure 2 to Figure S1), suggesting that our conclusions may apply even if some of the true parameters differ slightly from those used in our models.

Nevertheless, due to these inherent complexities in trying to jointly model African, African-American, and European population history, we also analyzed empirical data from African and African-American populations. The analyses of the NIEHS and Perlegen data allow us to test whether the predictions made from data generated under our simplified demographic models hold for data generated under the true demographic model of these populations. The fact that the growth parameters estimated using the SFS from the NIEHS data in the Yoruba and African-American populations were similar to each other, as predicted by our simulations, suggests that our simple models provide a reasonable guide to reality. Furthermore, the finding that the estimates of growth parameters using the HCN statistic from African-American data significantly differ from those estimated using the SFS is again consistent with the observations from our simulations.

These findings have implications for reconciling differences in estimates of population growth parameters made using African and African-American populations. Our finding from the NIEHS data of similar growth parameters for both the African-American and Yoruba individuals suggests that using African-American individuals as opposed to West African individuals should not lead to large differences in parameter estimates. Instead, we propose that the differences in estimates of growth parameters in different studies are likely to be due to differences in the amounts of natural selection in different data sets, systematic differences in laboratory protocols leading to different SFS among data sets, or differences in modeling methods (*e.g.*, whether or not migration is included) across studies. Consistent with this hypothesis, WALL *et al.* (2008) found that a summary of the SFS, Tajima's *D* (TAJIMA 1989b), significantly differed among different data sets consisting of West African populations. Further studies using more extensive resequencing data with similar laboratory protocols and more advanced demographic models will help obtain more consistent parameter estimates.

LITERATURE CITED

ADAMS, A. M., and R. R. HUDSON, 2004 Maximum-likelihood estimation of demographic parameters using the frequency spectrum of unlinked single-nucleotide polymorphisms. Genetics **168:** 1699–1712.

AKEY, J. M., M. A. EBERLE, M. J. RIEDER, C. S. CARLSON, M. D. SHRIVER *et al.*, 2004 Population history and natural selection shape patterns of genetic variation in 132 genes. PLoS Biol. **2:** e286.

BARBUJANI, G., and D. B. GOLDSTEIN, 2004 Africans and Asians abroad: Genetic diversity in Europe. Annu. Rev. Genomics Hum. Genet. **5:** 119–150.

BOYKO, A. R., S. H. WILLIAMSON, A. R. INDAP, J. D. DEGENHARDT, R. D. HERNANDEZ *et al.*, 2008 Assessing the evolutionary impact of amino acid mutations in the human genome. PLoS Genet. **4:** e1000083.

BRYC, K., A. AUTON, M. B. NELSON, J. R. OKSENBERG, S. L. HAUSER *et al.*, 2010 Genome-wide patterns of population structure and admixture in West Africans and African Americans. Proc. Natl. Acad. Sci. USA **107:** 786–791.

BUSTAMANTE, C. D., A. FLEDEL-ALON, S. WILLIAMSON, R. NIELSEN, M. T. HUBISZ *et al.*, 2005 Natural selection on protein-coding genes in the human genome. Nature **437:** 1153–1157.

CAICEDO, A. L., S. H. WILLIAMSON, R. D. HERNANDEZ, A. BOYKO, A. FLEDEL-ALON *et al.*, 2007 Genome-wide patterns of nucleotide polymorphism in domesticated rice. PLoS Genet. **3:** 1745–1756.

CAMPBELL, M. C., and S. A. TISHKOFF, 2008 African genetic diversity: implications for human demographic history, modern human origins, and complex disease mapping. Annu. Rev. Genomics Hum. Genet. **9:** 403–433.

CHAKRABORTY, R., and K. M. WEISS, 1988 Admixture as a tool for finding linked genes and detecting that difference from allelic association between loci. Proc. Natl. Acad. Sci. USA **85:** 9119–9123.

CLARK, A. G., 1990 Inference of haplotypes from PCR-amplified samples of diploid populations. Mol. Biol. Evol. **7:** 111–122.

COX, M. P., D. A. MORALES, A. E. WOERNER, J. SOZANSKI, J. D. WALL *et al.*, 2009 Autosomal resequence data reveal late stone age signals of population expansion in sub-Saharan African foraging and farming populations. PLoS One **4:** e6366.

FALUSH, D., M. STEPHENS and J. K. PRITCHARD, 2003 Inference of population structure using multilocus genotype data: linked loci and correlated allele frequencies. Genetics **164:** 1567–1587.

FU, Y. X., 1995 Statistical properties of segregating sites. Theor. Popul. Biol. **48:** 172–197.

GARRIGAN, D., and M. F. HAMMER, 2006 Reconstructing human origins in the genomic era. Nat. Rev. Genet. **7:** 669–680.

GRIFFITHS, R. C., and S. TAVARÉ, 1998 The age of a mutation in a general coalescent tree. Stoch. Models **14:** 273–295.

GUTENKUNST, R. N., R. D. HERNANDEZ, S. H. WILLIAMSON and C. D. BUSTAMANTE, 2009 Inferring the joint demographic history of multiple populations from multidimensional SNP frequency data. PLoS Genet. **5:** e1000695.

HERNANDEZ, R. D., M. J. HUBISZ, D. A. WHEELER, D. G. SMITH, B. FERGUSON *et al.*, 2007 Demographic histories and patterns of linkage disequilibrium in Chinese and Indian rhesus macaques. Science **316:** 240–243.

HINDS, D. A., L. L. STUVE, G. B. NILSEN, E. HALPERIN, E. ESKIN *et al.*, 2005 Whole-genome patterns of common DNA variation in three human populations. Science **307:** 1072–1079.

JAKOBSSON, M., S. W. SCHOLZ, P. SCHEET, J. R. GIBBS, J. M. VANLIERE *et al.*, 2008 Genotype, haplotype and copy-number variation in worldwide human populations. Nature **451:** 998–1003.

KEINAN, A., J. C. MULLIKIN, N. PATTERSON and D. REICH, 2007 Measurement of the human allele frequency spectrum demonstrates greater genetic drift in East Asians than in Europeans. Nat. Genet. **39:** 1251–1255.

LAUTENBERGER, J. A., J. C. STEPHENS, S. J. O'BRIEN and M. W. SMITH, 2000 Significant admixture linkage disequilibrium across 30

cM around the FY locus in African Americans. Am. J. Hum. Genet. **66:** 969–978.

LI, J. Z., D. M. ABSHER, H. TANG, A. M. SOUTHWICK, A. M. CASTO *et al.*, 2008 Worldwide human relationships inferred from genome-wide patterns of variation. Science **319:** 1100–1104.

LIND, J. M., H. B. HUTCHESON-DILKS, S. M. WILLIAMS, J. H. MOORE, M. ESSEX *et al.*, 2007 Elevated male European and female African contributions to the genomes of African American individuals. Hum. Genet. **120:** 713–722.

LIVINGSTON, R. J., A. VON NIEDERHAUSERN, A. G. JEGGA, D. C. CRAWFORD, C. S. CARLSON *et al.*, 2004 Pattern of sequence variation across 213 environmental response genes. Genome Res. **14:** 1821–1831.

LOHMUELLER, K. E., A. R. INDAP, S. SCHMIDT, A. R. BOYKO, R. D. HERNANDEZ *et al.*, 2008 Proportionally more deleterious genetic variation in European than in African populations. Nature **451:** 994–997.

LOHMUELLER, K. E., C. D. BUSTAMANTE and A. G. CLARK, 2009 Methods for human demographic inference using haplotype patterns from genomewide single-nucleotide polymorphism data. Genetics **182:** 217–231.

MARTH, G. T., E. CZABARKA, J. MURVAI and S. T. SHERRY, 2004 The allele frequency spectrum in genome-wide human variation data reveals signals of differential demographic history in three large world populations. Genetics **166:** 351–372.

NIELSEN, R., 2000 Estimation of population parameters and recombination rates from single nucleotide polymorphisms. Genetics **154:** 931–942.

NIELSEN, R., M. J. HUBISZ and A. G. CLARK, 2004 Reconstituting the frequency spectrum of ascertained single-nucleotide polymorphism data. Genetics **168:** 2373–2382.

NIELSEN, R., M. J. HUBISZ, I. HELLMANN, D. TORGERSON, A. M. ANDRES *et al.*, 2009 Darwinian and demographic forces affecting human protein coding genes. Genome Res. **19:** 838–849.

PARRA, E. J., A. MARCINI, J. AKEY, J. MARTINSON, M. A. BATZER *et al.*, 1998 Estimating African American admixture proportions by use of population-specific alleles. Am. J. Hum. Genet. **63:** 1839–1851.

PATTERSON, N., N. HATTANGADI, B. LANE, K. E. LOHMUELLER, D. A. HAFLER *et al.*, 2004 Methods for high-density admixture mapping of disease genes. Am. J. Hum. Genet. **74:** 979–1000.

PAWITAN, Y., 2001 *In All Likelihood: Statistical Modeling and Inference Using Likelihood.* Oxford University Press, Oxford.

PFAFF, C. L., E. J. PARRA, C. BONILLA, K. HIESTER, P. M. MCKEIGUE *et al.*, 2001 Population structure in admixed populations: effect of admixture dynamics on the pattern of linkage disequilibrium. Am. J. Hum. Genet. **68:** 198–207.

PLUZHNIKOV, A., A. DI RIENZO and R. R. HUDSON, 2002 Inferences about human demography based on multilocus analyses of non-coding sequences. Genetics **161:** 1209–1218.

PRICE, A. L., A. TANDON, N. PATTERSON, K. C. BARNES, N. RAFAELS *et al.*, 2009 Sensitive detection of chromosomal segments of distinct ancestry in admixed populations. PLoS Genet. **5:** e1000519.

PTAK, S. E., and M. PRZEWORSKI, 2002 Evidence for population growth in humans is confounded by fine-scale population structure. Trends Genet. **18:** 559–563.

REED, F. A., and S. A. TISHKOFF, 2006 African human diversity, origins and migrations. Curr. Opin. Genet. Dev. **16:** 597–605.

REINER, A. P., C. S. CARLSON, E. ZIV, C. IRIBARREN, C. E. JAQUISH *et al.*, 2007 Genetic ancestry, population sub-structure, and cardiovascular disease-related traits among African-American participants in the CARDIA study. Hum. Genet. **121:** 565–575.

SANKARARAMAN, S., G. KIMMEL, E. HALPERIN and M. I. JORDAN, 2008a On the inference of ancestries in admixed populations. Genome Res. **18:** 668–675.

SANKARARAMAN, S., S. SRIDHAR, G. KIMMEL and E. HALPERIN, 2008b Estimating local ancestry in admixed populations. Am. J. Hum. Genet. **82:** 290–303.

SCHAFFNER, S. F., C. FOO, S. GABRIEL, D. REICH, M. J. DALY *et al.*, 2005 Calibrating a coalescent simulation of human genome sequence variation. Genome Res. **15:** 1576–1583.

SELDIN, M. F., T. MORII, H. E. COLLINS-SCHRAMM, B. CHIMA, R. KITTLES *et al.*, 2004 Putative ancestral origins of chromosomal segments in individual African Americans: implications for admixture mapping. Genome Res. **14:** 1076–1084.

SLATKIN, M., and R. R. HUDSON, 1991 Pairwise comparisons of mitochondrial DNA sequences in stable and exponentially growing populations. Genetics **129:** 555–562.

STADLER, T., B. HAUBOLD, C. MERINO, W. STEPHAN and P. PFAFFELHUBER, 2009 The impact of sampling schemes on the site frequency spectrum in nonequilibrium subdivided populations. Genetics **182:** 205–216.

TAJIMA, F., 1989a The effect of change in population size on DNA polymorphism. Genetics **123:** 597–601.

TAJIMA, F., 1989b Statistical method for testing the neutral mutation hypothesis by DNA polymorphism. Genetics **123:** 585–595.

TANG, H., M. CORAM, P. WANG, X. ZHU and N. RISCH, 2006 Reconstructing genetic ancestry blocks in admixed individuals. Am. J. Hum. Genet. **79:** 1–12.

TIAN, C., D. A. HINDS, R. SHIGETA, R. KITTLES, D. G. BALLINGER *et al.*, 2006 A genomewide single-nucleotide-polymorphism panel with high ancestry information for African American admixture mapping. Am. J. Hum. Genet. **79:** 640–649.

TISHKOFF, S. A., and S. M. WILLIAMS, 2002 Genetic analysis of African populations: human evolution and complex disease. Nat. Rev. Genet. **3:** 611–621.

VOIGHT, B. F., A. M. ADAMS, L. A. FRISSE, Y. QIAN, R. R. HUDSON *et al.*, 2005 Interrogating multiple aspects of variation in a full resequencing data set to infer human population size changes. Proc. Natl. Acad. Sci. USA **102:** 18508–18513.

WALL, J. D., M. P. COX, F. L. MENDEZ, A. WOERNER, T. SEVERSON *et al.*, 2008 A novel DNA sequence database for analyzing human demographic history. Genome Res. **18:** 1354–1361.

WALL, J. D., K. E. LOHMUELLER and V. PLAGNOL, 2009 Detecting ancient admixture and estimating demographic parameters in multiple human populations. Mol. Biol. Evol. **26:** 1823–1827.

WILLIAMSON, S. H., R. HERNANDEZ, A. FLEDEL-ALON, L. ZHU, R. NIELSEN *et al.*, 2005 Simultaneous inference of selection and population growth from patterns of variation in the human genome. Proc. Natl. Acad. Sci. USA **102:** 7882–7887.

XU, S., W. HUANG, H. WANG, Y. HE, Y. WANG *et al.*, 2007 Dissecting linkage disequilibrium in African-American genomes: roles of markers and individuals. Mol. Biol. Evol. **24:** 2049–2058.

ZHU, L., and C. D. BUSTAMANTE, 2005 A composite-likelihood approach for detecting directional selection from DNA sequence data. Genetics **170:** 1411–1421.

Communicating editor: A. DI RIENZO

GENETICS

The Effect of Recent Admixture on Inference
of Ancient Human Population History

Kirk E. Lohmueller, Carlos D. Bustamante and Andrew G. Clark
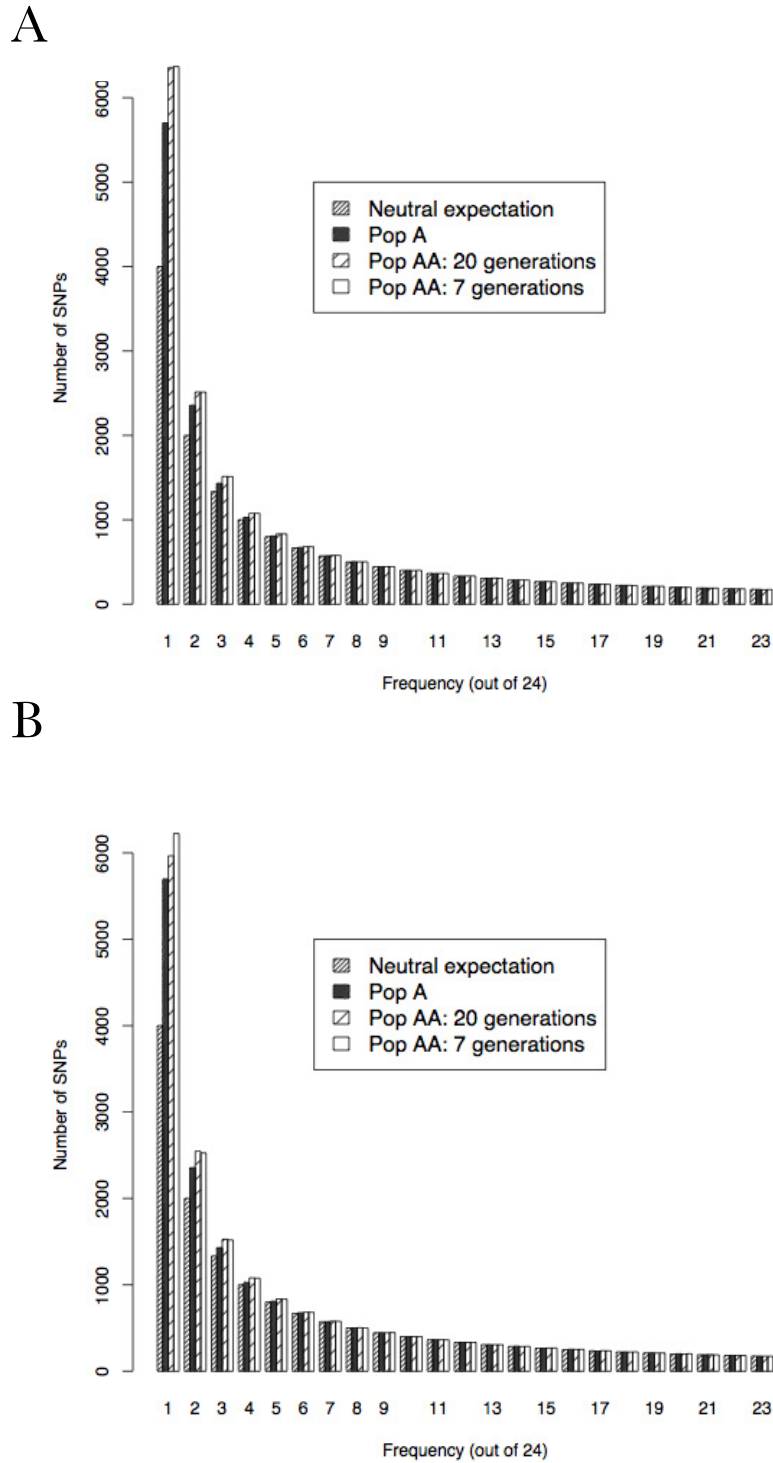
A

B

FIGURE S1.—Expected SFS in a sample size of 24 chromosomes for Pop A and Pop AA under population growth when admixture occurs 20 or 7 generations ago. Note in both cases, the SFS when admixture occurs 20 generations ago is similar to that when admixture occurs 7 generations ago. (A) $\mathcal{N}_{AA} = \mathcal{N}_A$ and (B) $\mathcal{N}_{AA} = 0.1\mathcal{N}_A$. Overall there is a slight excess of singletons when admixture occurs 7 generations ago as opposed to 20 generations ago, since there is less drift in Pop AA with the more recent founding. However, the number of singletons in Pop AA when $\mathcal{N}_{AA} = 0.1\mathcal{N}_A$ is still less than that when $\mathcal{N}_{AA} = \mathcal{N}_A$. $\mathcal{N}_A = 20{,}000$; $\mathcal{N}_B/\mathcal{N}_A = 0.5$; $t_{cur} = 2400$ generations.
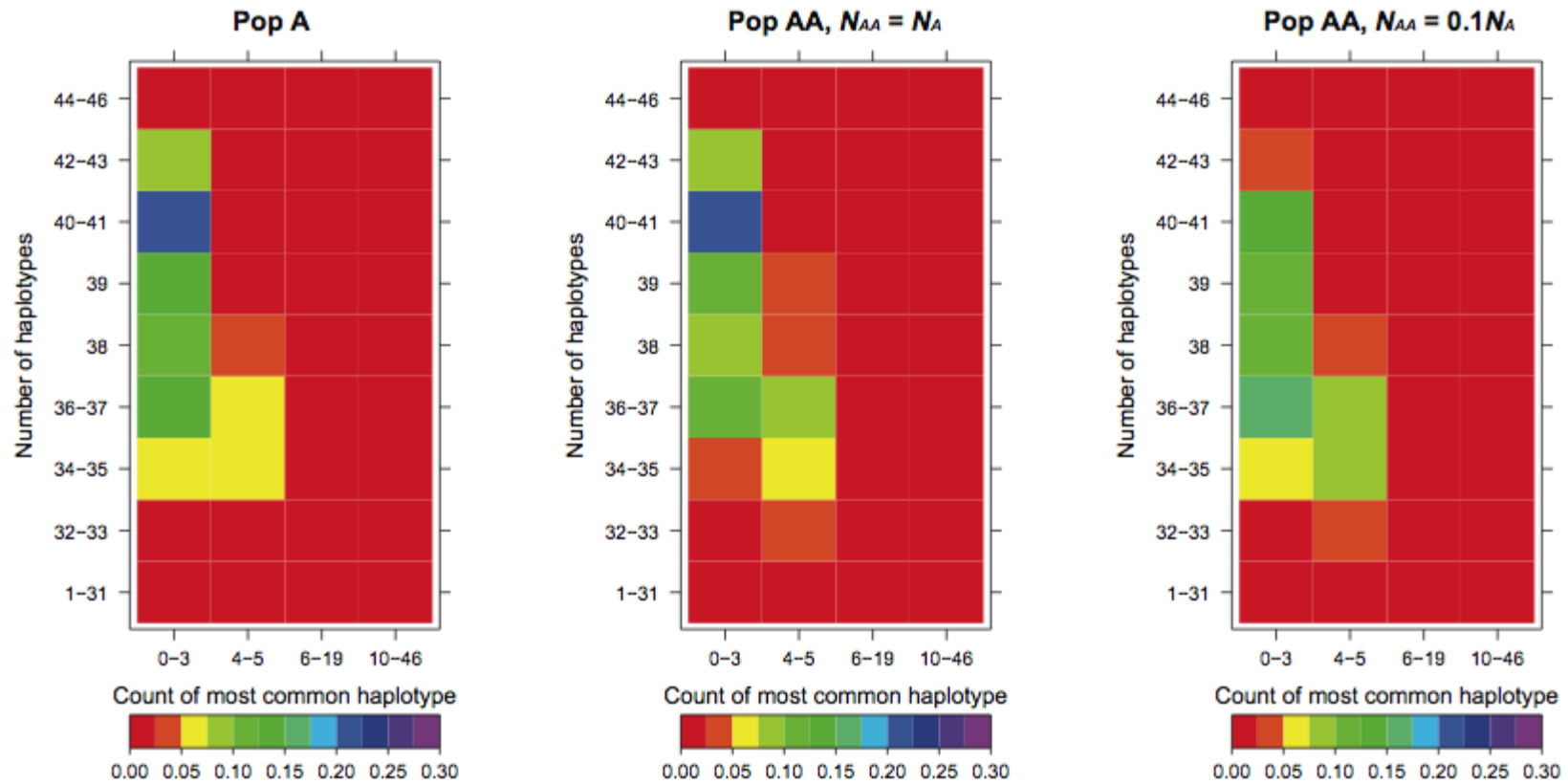
FIGURE S2.—Expected HCN statistic for population growth (Pop A) and for growth with admixture (Pop AA) when admixture occurred 7 generations ago (instead of 20 generations). Each cell in the matrix is colored according to the proportion of simulation replicates (windows) having the particular configuration of the number of haplotypes and count of the most common haplotype. For example, red cells contain <2.5% of windows and medium-blue cells contain 20-22.5% of simulated windows. Note the excess of windows with fewer haplotypes and where the most common haplotype is at higher frequency in Pop AA relative to Pop A. This is most pronounced when $N_{AA} = 0.1 N_A$. Note, the simulations assume $N_A = 20,000$; $N_B/N_A = 0.5$; $t_{cur} = 2400$ generations.
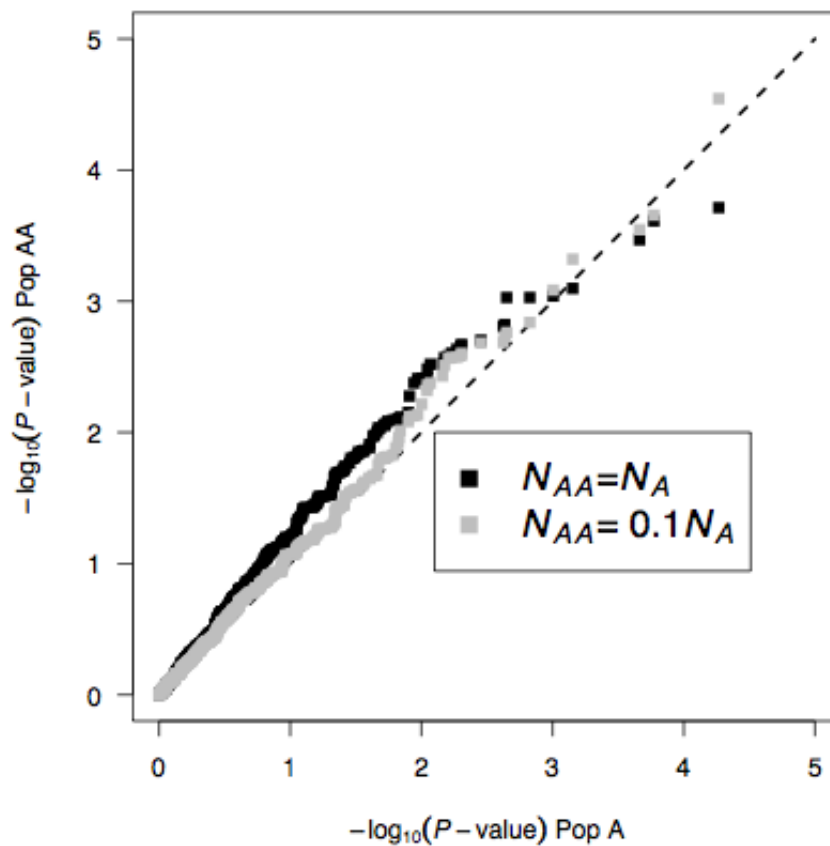
FIGURE S3.—Quantile-Quantile (*Q-Q*) plot comparing the chi-square goodness of fit test *P*-values from data simulated from Pop A (*x*-axis) and Pop AA (*y*-axis). Note the excess of lower *P*-values in Pop AA relative to Pop A for both values of N_{AA}. These results suggest that the best-fitting growth parameters tend to fit Pop AA (where the true demographic model involves admixture) slightly worse than they do for Pop A (where the true demographic model is a growth model). Here $t_{cur} = 2400$ generations.
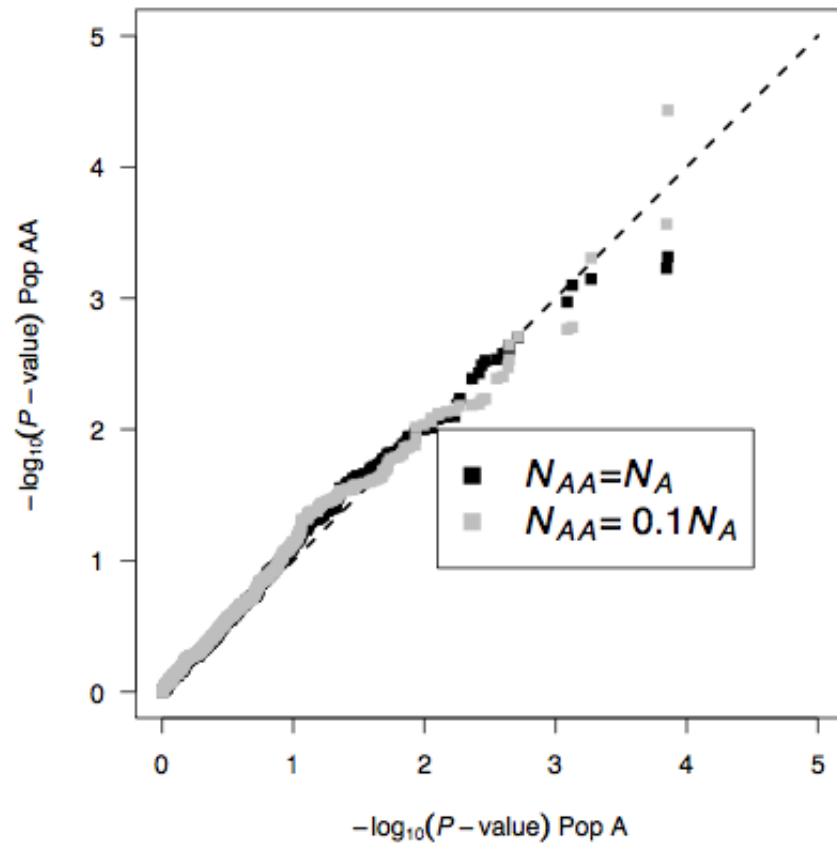
FIGURE S4.—Quantile-Quantile (*Q-Q*) plot comparing the chi-square goodness of fit test *P*-values from data simulated from Pop A (*x*-axis) and Pop AA (*y*-axis). Note that there is not as much of an excess of low *P*-values for Pop AA as there was in Supplementary Figure 2. Here t_{cur} = 4000 generations.
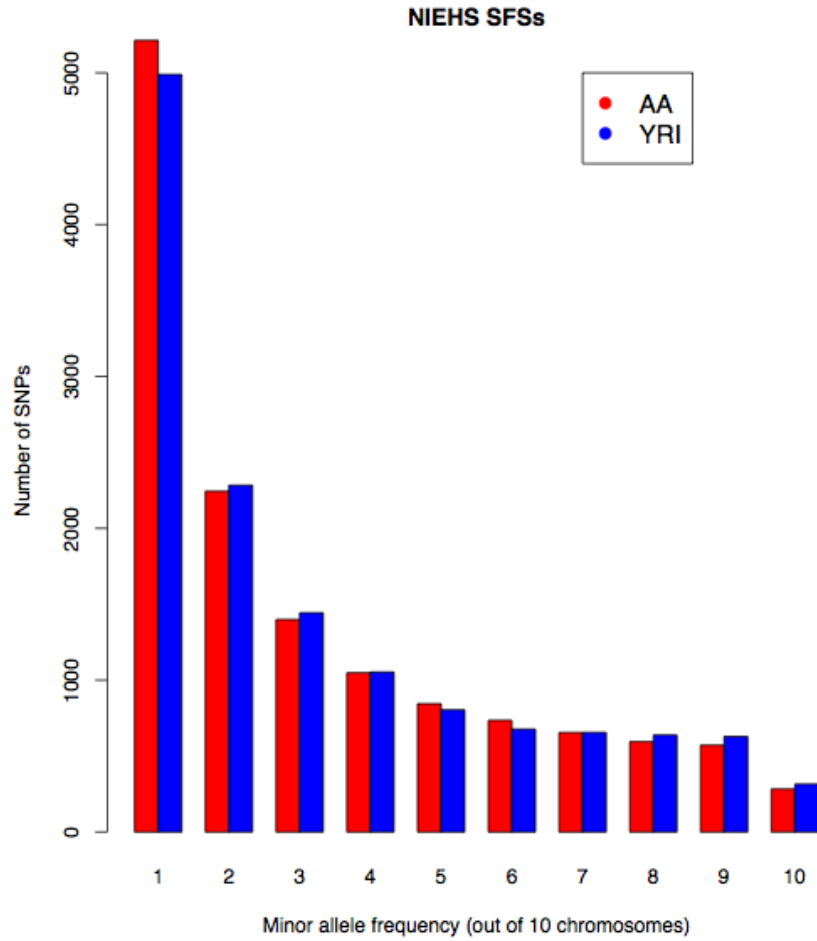
FIGURE S5.—The folded SFS for the Yoruba (YRI) and African American (AA) samples in the NIEHS data set. The folded SFS presents the number of SNPs where the minor allele has a given frequency. Note, to allow for missing data, we projected the SFS to a sample size of 20 chromosomes.
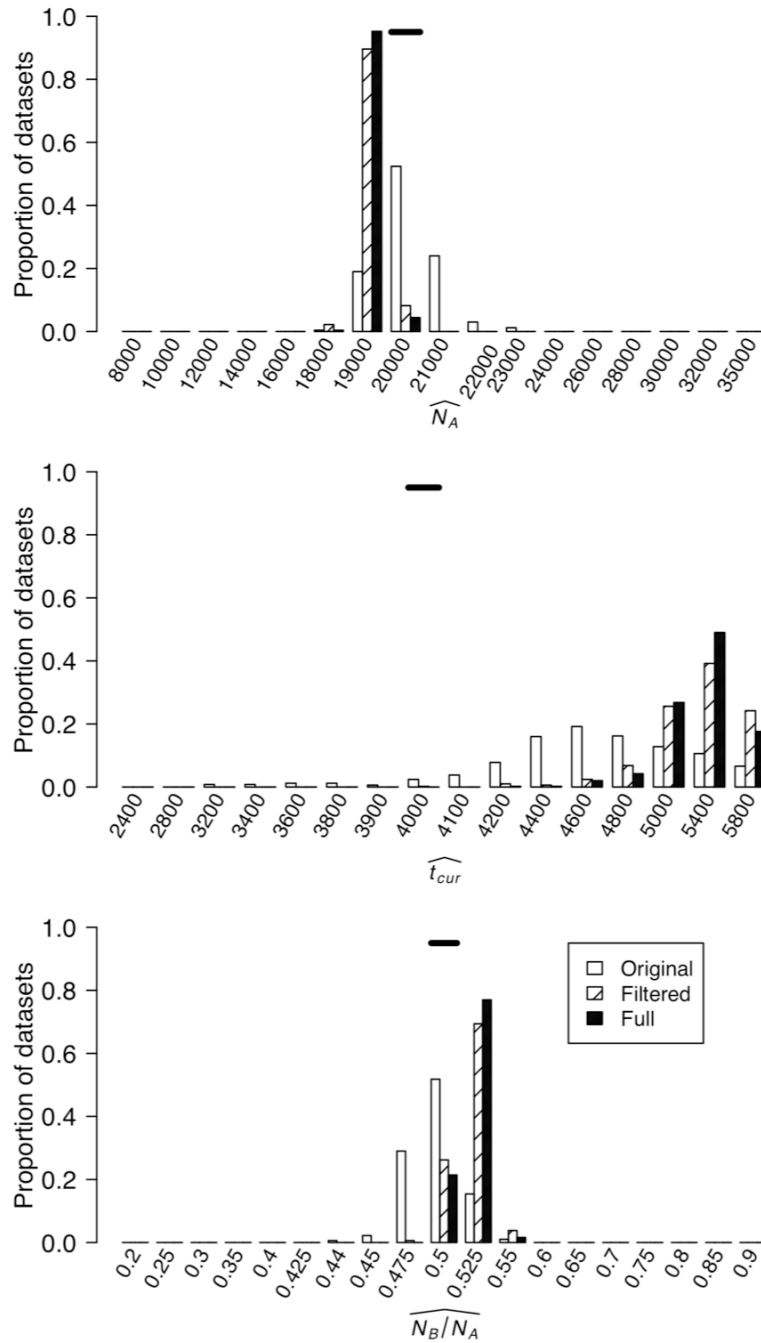
FIGURE S6.— Distribution of MLEs for the three growth parameters inferred using the SFS from Pop AA using different size data sets. "Original" denotes the original data sets presented in Figure 5 using a sample size of $n = 24$ chromosomes. "Filtered" denotes data sets consisting of a sample size of $n = 100$ chromosomes. Here we filtered SNPs so that the number of SNPs per data set was approximately equal to the mean number of SNPs in the original data sets. "Full" denotes the data sets consisting of a sample size of $n = 100$ without filtering any SNPs. Solid horizontal bars denote the true parameter values for Pop A ($N_A = 20{,}000$; $N_B / N_A = 0.5$; $t_{cur} = 4000$ generations).